Cardiovascular Intervention and Therapeutics (2023) 38:86–95
https://doi.org/10.1007/s12928-022-00880-0

ORIGINAL ARTICLE

Identification of post-procedural optical coherence tomography findings associated with the 1-year vascular response evaluated by coronary angioscopy

Naoko Higashino[1] · Takayuki Ishihara[1] · Osamu Iida[1] · Takuya Tsujimura[1] · Yosuke Hata[1] · Taku Toyoshima[1] · Sho Nakao[1] · Naoya Kurata[2] · Toshiaki Mano[1]

Received: 22 January 2022 / Accepted: 18 July 2022 / Published online: 2 August 2022
© The Author(s) under exclusive licence to Japanese Association of Cardiovascular Intervention and Therapeutics 2022

Abstract

Optical coherence tomography (OCT) provides higher resolution intravascular imaging and allows detailed evaluations of stent implantation sites post-percutaneous coronary intervention (PCI). Coronary angioscopy (CAS) can evaluate the vascular response after drug-eluting stent (DES) implantation. The post-PCI OCT findings that are associated with the CAS 1-year vascular response have not been known. We enrolled 168 lesions from 119 patients who underwent OCT-guided PCI using DES and follow-up CAS observation at 1 ± 0.5 year from August 2012 to December 2019. Outcome measures were sufficient neointimal coverage (NIC) defined as stent struts embedded in the neointima, subclinical intrastent thrombus, and vulnerable stented segments defined as those with angioscopic yellow or intensive yellow color 1 year after PCI. We identified the post-PCI OCT findings associated with these CAS findings. Sufficient NIC, subclinical intrastent thrombus, and vulnerable stented segment were detected in 85 lesions (51%), 47 lesions (28%), and 54 lesions (32%), respectively. A multivariate analysis demonstrated that malapposed struts were negatively associated with sufficient NIC (odds ratio 0.87; 95% CI 0.76–0.99; $p = 0.029$). However, no specific OCT findings immediately after PCI were associated with subclinical intrastent thrombus or vulnerable stented segment. Malapposition immediately after PCI was negatively associated with sufficient NIC at 1 year even without associations between post-PCI OCT findings and subclinical intrastent thrombus or vulnerable stented segment.

Keywords Coronary angioscopy · Malapposition · Optical coherence tomography · Thrombus

Abbreviations

CAS	Coronary angioscopy
CRP	C-reactive protein
DES	Drug-eluting stent
ISA	Incomplete stent apposition
LAD	Left anterior descending
NIC	Neointimal coverage
OCT	Optical coherence tomography
PCI	Percutaneous coronary intervention
SED	Stent edge dissection
ST	Stent thrombosis

Introduction

The incidences of late and very late stent thrombosis (ST) after the implantation of a drug-eluting stent (DES) have been decreasing in the second-generation DES era, but the ST issue has not been resolved completely [1]. The main causes of late and very late ST are delayed healing and abnormal vascular response [2]. To assess the risk of ST, it is informative to evaluate the intravascular status using intravascular imaging.

Coronary angioscopy (CAS) can evaluate vascular responses such as the neointimal coverage (NIC), the presence/absence of an intrastent thrombus, and yellow color of the stented segment with real image and full color. Classically, poor NIC (which has been judged as uncovered struts demonstrated by pathological and optical coherence tomography [OCT]) was an independent predictor of ST [3, 4]. In a case with very late ST 5 years after first-generation sirolimus-eluting stent, CAS demonstrated that stent struts

✉ Takayuki Ishihara
t.ishihara31@gmail.com

[1] Kansai Rosai Hospital Cardiovascular Center, 3-1-69 Inabaso, Amagasaki, Hyogo 660-8511, Japan

[2] Department of Clinical Engineering, Kansai Rosai Hospital, Amagasaki, Japan

were uncovered and fully visible [5]. Compared to OCT, CAS is better able to detect thrombi [6]. Since thrombus adhesion is an initial phase of arterial repair and does not occur where arterial repair is complete, thrombus adhesion is considered an indicator of delayed arterial healing [7, 8]. Because the intensity of yellow color is negatively correlated with the thickness of the fibrous cap, intense yellow color indicates high plaque vulnerability [9]. In addition, the previous article which mentioned that coronary endothelial dysfunction was associated with poor neointimal coverage after DES implantation suggested the accuracy of CAS as a surrogate marker of arterial healing [10].

Compared to the other types of intravascular imaging OCT provides high-resolution images, and thus OCT is useful for the guidance of percutaneous coronary intervention (PCI). In an OCT-guided PCI, the precise intravascular status immediately after the implantation of DES can be determined [11, 12]. Several previous studies with serial OCT observations showed that acute-phase stent findings such as stent malapposition or protrusions were associated with chronic-phase suboptimal intrastent findings after DES implantation [13–16]. However, the association between acute-phase post-PCI OCT findings and chronic-phase vessel responses evaluated by CAS after DES implantation has not been elucidated. We conducted the present study to identify the post-PCI OCT findings that are associated with 1-year CAS findings.

Methods

Patients

This was a single-center, retrospective observational study. We enrolled the cases of patients who received an OCT-guided PCI and follow-up CAS observation 1 ± 0.5 year after the PCI during the period from August 2012 to December 2019 at Kansai Rosai Hospital. All DESs were implanted in de novo lesions in native coronary arteries. We excluded the cases of patients without OCT imaging immediately after PCI and patients with poor image quality, incomplete imaging of the entire stent length, and those in whom a covered stent was used. We also excluded patients who exhibited any event of stent failure before CAS observation such as in-stent restenosis, and those who did not undergo a successful angioscopic evaluation (Fig. 1).

Although CAS observation at follow-up angiography as well as staged PCI for other lesions was recommended for all patients, this was not performed when informed consent could not be obtained, or when a specialist for angioscopic evaluation was not available. A final total of 168 lesions from 119 patients were included in the analysis. The elective patients received ticlopidine (200 mg/day), clopidogrel (75 mg/day), or prasugrel (3.75 mg/day) in addition to aspirin (100 mg/day) at ≥ 1 week before their PCI. For the emergent patients, the antiplatelet drugs (aspirin 200 mg and clopidogrel 300 mg or prasugrel 20 mg) were loaded before

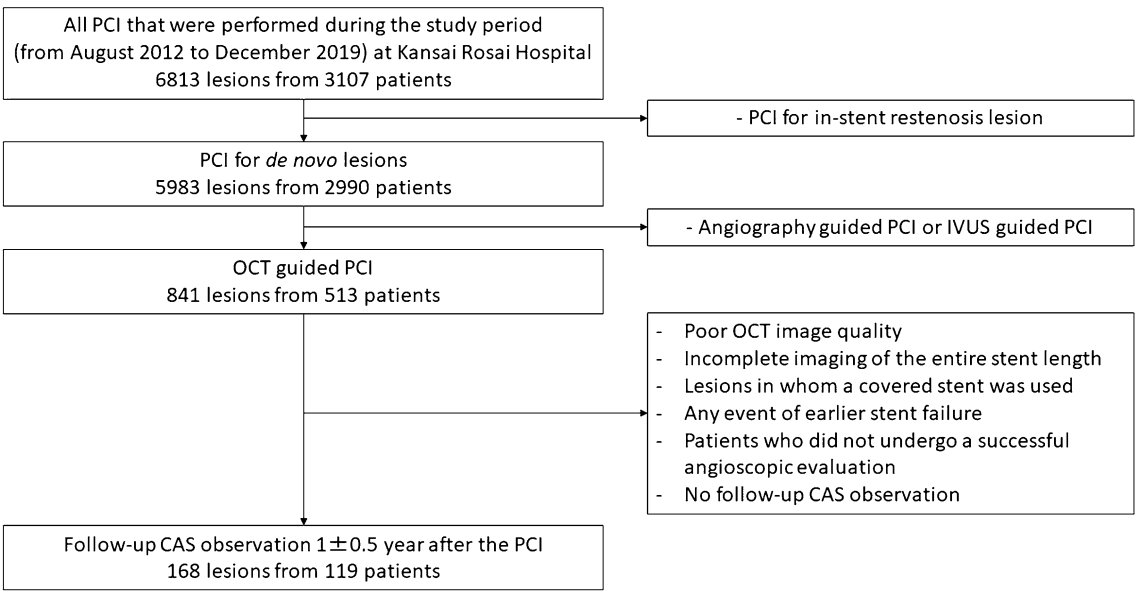

Fig. 1 Study flowchart. A total of 6813 lesions from 3107 patients underwent PCI from the study period in our hospital. Of these, 5983 lesions from 2990 patients were de novo lesions, and OCT-guided PCI was performed for 841 lesions from 513 patients. Follow-up CAS observation was performed for 168 lesions from 119 patients 1 ± 0.5 year after the PCI. *CAS* coronary angioscopy; *IVUS* intravascular ultrasound; *OCT* optical coherence tomography; *PCI* percutaneous coronary intervention

the PCI. Dual-antiplatelet therapy was continued according to the guideline at that time. The Medical Ethics Committee of Kansai Rosai Hospital approved the study (Reference number: 18D060g), and all patients provided written informed consent.

OCT image acquisition and analysis

The methodology that we used herein for the OCT evaluation was decided based on a previous report [17, 18]. We analyzed the cross-section for every 1 mm of OCT imaging immediately after the respective patient's PCI. OCT images spanning the entire length of the stent plus 5-mm-proximal and 5-mm-distal reference segments were analyzed. The qualitative analysis included evaluations for stent edge dissection (SED), in-stent dissection, incomplete stent apposition (ISA), in-stent tissue protrusion (smooth protrusion, disrupted fibrous tissue protrusion, and irregular protrusion), and thrombus. For the qualitative analysis, we analyzed all of the cross-sectional images within the entire stent length and 5-mm peri-stent segments.

When > 2 consecutive frames were not analyzable due to residual blood or artifacts, the case was considered to have poor image quality and was, therefore, excluded. SED was defined as the disruption of the vessel luminal surface with a visible flap at the stent edge or at the 5-mm proximal and distal reference segments. When a dissection flap was visualized, the maximum flap length (mm) on the cross-sectional view and the dissection length (mm) on the longitudinal view were recorded. In-stent dissection was defined as disruption of the luminal vessel surface within the stented segment. ISA was defined as separation of the inner surface of a stent strut from the inner vessel wall, in segments without a side branch, by a distance greater than or equal to the axial resolution of OCT plus the width of the stent strut of each stent type including the polymer coating.

For quantitative parameters of ISA, we counted the number of total struts and malapposed struts and measured the strut-to-vessel wall distance (S–V distance, mm), defined as the distance between the inner surface of the stent strut and the inner surface of the vessel wall for each cross-section. The maximum S–V distance was recorded for each lesion. We recorded the malapposition area for each cross-section; the malapposition volume was defined as the sum of the malapposition areas multiplied by the analysis length. We defined '%malapposed struts' as the number of malapposed struts divided by the total number of struts.

In-stent tissue protrusion was divided into three categories: smooth protrusion, disrupted fibrous tissue protrusion, and irregular protrusion. Smooth protrusion was defined as the bowing of plaque into the lumen between stent struts, without intimal disruption, appearing as a smooth semicircular arc connecting adjacent struts, and likely representing the compression of soft plaque by the stent. Disrupted fibrous tissue protrusion was defined as disruption of underlying fibrous tissue protruding in between stent struts into the lumen. Irregular protrusion was defined as protrusion of material with an irregular surface into the lumen between stent struts. Thrombus was defined as a mass with a diameter ≥ 250 μm attached to the luminal surface, stent strut, or floating within the lumen. When thrombus could not be completely differentiated from irregular protrusion, we categorized it as irregular protrusion.

For the quantitative evaluation, we analyzed cross-sectional OCT images at 1.0-mm intervals for the following parameters: maximum, minimum, and mean stent diameter; stent area; maximum, minimum, and mean lumen diameter; lumen area; maximum, minimum, and mean reference diameter (largest lumen within 5 mm of the proximal and distal edges); and the reference area (within 5 mm of the proximal and distal edges). We identified stent underexpansion as a ratio of the minimum stent area (MSA) to the mean reference area at < 0.8.

CAS follow-up

CAS was performed after the administration of unfractionated heparin (5000 IU) into the radial or femoral artery via the inserted sheath and the administration of isosorbide dinitrate into the coronary artery. CAS was subsequently performed using a Fullview NEO angioscopic catheter (FiberTech, Tokyo) during the period from August 2012 to September 2016. Briefly, an optical fiber was placed at the distal segment of the coronary artery and manually pulled back from the distal edge of the stent to the proximal edge under careful angioscopic and angiographic guidance. Since October 2016, we have been using a smart-i angioscopic catheter (i Heart Medical, Tokyo) because the Fullview NEO was discontinued. Using guide extension catheters such as the GuideLiner (Japan Lifeline, Tokyo), Guidezilla (Boston Scientific, Natick, MA, USA), and Guideplus (NIPRO, Osaka, Japan), we blocked blood flow by flushing with low-molecular-weight dextran. Both angioscopic images consisted of 3000 pixels with full color and were digitally stored for off-line analysis.

CAS analysis

CAS images were analyzed to determine the following: (1) the dominant degree of neointimal coverage (NIC) over the stent, (2) the presence/absence of a subclinical intrastent thrombus, and (3) the yellow color grade of the stented segment. NIC over the stent was classified into four grades as described [19]: grade 0, stent struts fully visible, similar to immediately after implantation; grade 1, stent struts bulging into the lumen and although covered, still transparently

visible; grade 2, stent struts embedded in the neointima, but translucently visible; and grade 3, stent struts fully embedded and invisible on angioscopy.

NIC that was ≥ grade 2 was defined as sufficient NIC. Subclinical intrastent thrombus was defined as a material adhering to the luminal surface or protruding into the lumen [20]. The yellow color was graded as follows: grade 0, white; grade 1, light yellow; grade 2, yellow; grade 3, intensive yellow [21]. Yellow color that was ≥ grade 2 was defined as indicating a vulnerable stented segment. As mentioned in a previous article from our institution [21], the estimated inter- and intra-observer k-coefficients were 0.84 and 0.95, respectively, for the dominant degree of NIC over the stent; 0.93 and 1.0 for the presence of subclinical intrastent thrombus; and 0.82 and 0.86 for the yellow color grade of the stented segment.

Study outcomes

The outcome measures were sufficient NIC, the presence/absence of subclinical intrastent thrombus, and the presence/absence of vulnerable stented segment(s) evaluated by CAS at 1 year post-PCI. We evaluated the post-PCI OCT findings associated with these CAS findings.

Statistical analysis

All results are expressed as the mean ± SD (standard deviation) unless otherwise stated. Continuous variables with and without homogeneity of variance were analyzed by Student's *t* test and Welch's *t* test, respectively. Categorical variables were analyzed with Fisher's exact test for 2 × 2 comparisons. The multivariate analysis was performed with a logistic regression analysis. Variables in the univariate analysis with *p* values < 0.05 were selected for the multivariate analysis. Statistical significance was defined as $p < 0.05$. All calculations were performed using the IBM SPSS Statistics package ver. 26 (IBM, Armonk, NY).

Results

Patients

The patients' characteristics and medications at the time of their follow-up CAS observation are summarized in Table 1. Of the 119 patients, 107 patients (89.9%) were male, and the mean age was 70 ± 10 years old. Notable comorbidities included hypertension (87 patients, 73.1%), dyslipidemia (91 patients, 76.5%), and diabetes mellitus (50 patients, 42.0%). Eighty-one patients (68.1%) were being treated with a P2Y12 inhibitor, and 82 patients (68.9%) were being treated with a statin. Dual-antiplatelet therapy continued for 102 patients (85.7%).

Table 1 Patient characteristics ($n = 119$)

Male, *n* (%)	107 (89.9)
Age, years	70 ± 10
Hypertension, *n* (%)	87 (73.1)
Dyslipidemia, *n* (%)	91 (76.5)
Diabetes, *n* (%)	50 (42.0)
Smoking, *n* (%)	44 (37.0)
Hemodialysis, *n* (%)	1 (0.84)
Aspirin, *n* (%)	114 (95.8)
P2Y12 inhibitor, *n* (%)	81 (68.1)
Dual antiplatelet therapy, *n* (%)	102 (85.7)
Statin, *n* (%)	82 (68.9)
DOAC, *n* (%)	4 (3.36)

Data are mean ± SD or number (%)

DOAC direct oral anticoagulant

Table 2 Lesion and procedural characteristics ($n = 168$)

Target vessel, *n* (%)	
Left anterior descending artery	76 (45.2)
Left circumflex artery	42 (26.8)
Right coronary artery	50 (29.8)
Type B2/C, *n* (%)	134 (79.8)
Bifurcation, *n* (%)	73 (43.5)
Chronic total occlusion, *n* (%)	4 (2.38)
Calcification, *n* (%)	39 (23.2)
Acute coronary syndrome, *n* (%)	17 (10.1)
Second-generation drug-eluting stent, *n* (%)	36 (21.4)
Third-generation drug-eluting stent, *n* (%)	47 (28.0)
Newer-generation drug-eluting stent, *n* (%)	10 (6.0)
Drug-coated stent, *n* (%)	75 (44.6)
Pre-dilatation balloon maximum diameter, mm	2.65 ± 0.47
Pre-dilatation balloon maximum inflation pressure, atm	13.1 ± 3.02
Maximum stent diameter, mm	3.00 ± 0.46
Minimum stent diameter, mm	2.93 ± 0.48
Stent implantation pressure, atm	8.87 ± 2.74
Post-dilatation balloon maximum diameter, mm	3.29 ± 0.51
Post-dilatation balloon maximum inflation pressure, atm	16.2 ± 3.40

Data are mean ± SD or number (%)

The lesion and procedural characteristics are shown in Table 2. Among the 168 lesions, 76 lesions (45.2%) were left anterior descending (LAD) lesions, 134 lesions (79.8%) were Type B2/C, and 17 lesions (10.1%) were acute coronary syndrome (ACS) lesions. The following mean values were obtained: pre-dilatation balloon maximum diameter, 2.65 ± 0.47 mm; maximum stent diameter, 3.00 ± 0.46 mm; minimum stent diameter, 2.93 ± 0.48 mm; and post-dilatation

balloon maximum diameter, 3.29 ± 0.51 mm. There were 36 lesions with second-generation DES (3 lesions: Promus®, Boston Scientific; 4 lesions: Resolute®, Medtronic, Minneapolis, MN; 29 lesions: Xience®, Abbott Vascular, Abbott Park, IL), 47 lesions with third-generation DES (40 lesions: Synergy®, Boston Scientific; 7 lesions: Ultimaster®, Terumo, Tokyo), 10 lesions with newer generation DES (Orsiro®, Biotronik, Bülach, Switzerland), and 75 lesions treated with Drug-coated stent (BioFreedom®, Biosensors Interventional Technologies, Singapore).

CAS findings

Sufficient NIC was detected in 85 lesions (51%), subclinical intrastent thrombus was detected in 47 lesions (28%), and vulnerable stented segment was detected in 54 lesions (3%). Table 3 lists the predictors of sufficient coverage (NIC ≥ 2) at 1 year after PCI. After the multivariate analysis, the %malapposed struts was negatively associated with sufficient coverage (odds ratio [OR] 0.87; 95% confidence interval [CI] 0.76–0.99; $p = 0.029$). The predictors of thrombus adhesion at 1 year post-PCI are shown in Table 4. Pre-PCI C-reactive protein (CRP) level was positively associated with a subclinical intrastent thrombus at 1 year. However, in terms of the OCT findings immediately after PCI, while the malapposition volume showed a tendency for a positive correlation, no findings immediately post-PCI predicted a subclinical intrastent thrombus at 1 year. Table 5 provides the predictors of a vulnerable stented segment 1 year post-PCI. After the multivariate analysis, no findings immediately after PCI predicted a vulnerable stented segment at 1 year. Table 6 provides the difference of response after DES implantation according to the stent types. There was no significant difference of vascular response after DES implantation according to the stent types. Furthermore, after logistic regression analysis, no type of stents showed a significant differences of vascular response after DES implantation compared to the second-generation DES (Tables 3, 4, 5). In addition, there was no significant association between dual-antiplatelet therapy and the presence of a subclinical intrastent thrombus (OR 0.59; 95% CI 0.23–1.52; $p = 0.27$). Similarly, there was no significant association with a subclinical intrastent thrombus for statins (OR 1.27; 95% CI 0.50–3.21; $p = 0.61$) and direct oral anticoagulant (OR 1.03; 95% CI 0.19–5.51; $p = 0.97$).

Discussion

Through the evaluation of second- and later generation DESs, we determined the following in this study: (1) there was a significant association between %malapposition immediately after PCI and sufficient NIC at 1 year post-PCI; (2) there was no association between OCT findings immediately after PCI and the incidence of subclinical intrastent thrombus or vulnerable stented segment 1 year post-PCI.

Previous OCT studies demonstrated the association between malapposition immediately after PCI and poor strut coverage [13–15]. The current study in which CAS was used to evaluate the chronic-phase neointimal coverage is consistent to the previous serial OCT studies. Smooth muscle cell proliferation occurs at a stented site contacting the vessel wall [7]. It is thus difficult for neointima to cover a stent implantation site with severe malapposition, as neointima is composed mainly of smooth muscle cells, and our present analyses revealed that the %malapposition was a negative independent predictor for sufficient NIC. Insufficient NIC would have an impact on the risk of ST [3, 4], and it is important to confirm the adequate strut apposition at the time when the PCI is performed, to obtain future better future NIC.

Subclinical intrastent thrombi observed by CAS at 9 months after the implantation of second-generation DESs was independently associated with future major adverse clinical events [22]. Since intrastent thrombus is a marker of endothelial dysfunction [10], a patient's unique endothelial dysfunction would contribute to the relationship between subclinical intrastent thrombus and the future clinical outcome. Several OCT studies demonstrated that malapposition was one of the major causes of stent thrombosis [23–25]. However, in our present investigation, only the malapposition volume had a tendency to be associated with the presence of a subclinical thrombus (without statistical significance). Lee et al. reported that OCT-guided PCI resulted in a lower proportion of uncovered struts compared to angiography-guided PCI [26]. Since we routinely perform OCT-guided PCI and decrease the malapposition as much as possible, this could have contributed to the decrease in the absolute incidence of malapposition, which may lead to an insufficient sample size and decrease the statistical power. On the contrary, pre-PCI CRP level was positively associated with a subclinical intrastent thrombus at 1 year. Sakai et al. revealed in the article of in vivo evaluation of tissue protrusion by OCT and CAS immediately after PCI that the incidence of thrombus was most frequent in the irregular protrusion group and the increase in high-sensitivity CRP levels after stent implantation was significantly more frequent in the irregular protrusion than in the other protrusion groups [27]. Judging from these findings, there would be a relationship between thrombus adhesion and inflammation. Precise mechanism of the relationship between pre-PCI CRP level and thrombus adhesion in the chronic phase is unknown, and further investigation is necessary.

Miyoshi et al. revealed the relationship between OCT-tissue protrusion and the CAS-yellow plaque grade immediately after stent implantation [28]. Although two CAS

Table 3 Logistic regression analysis for sufficient neointimal coverage (≥ grade 2)

	Univariate			Multivariate		
	OR	95% CI	*p*-value	OR	95% CI	*p*-value
Male	0.63	0.19–2.10	0.45			
Age (1 year increase)	0.99	0.96–1.02	0.55			
BMI (1 kg/m^2 increase)	1.05	0.96–1.15	0.32			
Hypertension	0.75	0.38–1.52	0.43			
Dyslipidemia	0.78	0.36–1.66	0.52			
Diabetes mellitus	1.17	0.63–2.17	0.62			
HbA1c (1% increase)	1.18	0.88–1.58	0.27			
LDL-Cholesterol (1 mg/dl increase)	1.00	0.99–1.01	0.68			
CRP (1 mg/dl increase)	0.84	0.30–2.33	0.74			
HbA1c at follow-up phase (1% increase)	1.17	0.88–1.55	0.28			
LDL-Cholesterol at follow-up phase (1 mg/dl increase)	1.00	0.99–1.01	0.69			
CRP at follow-up phase (1 mg/dl increase)	0.15	0.02–1.40	0.10			
Aspirin[a]	2.49	0.63–9.85	0.20			
Clopidogrel[a]	0.96	0.39–2.35	0.93			
Prasugrel[a]	1.13	0.52–2.47	0.76			
Ticlopidine[a]	0.48	0.04–5.35	0.55			
Statin[a]	0.60	0.30–1.21	0.15			
Follow-up duration (1 day increase)	1.00	0.99–1.00	0.89			
Acute coronary syndrome	0.85	0.31–2.33	0.76			
Pre-dilatation balloon maximum diameter (1 mm increase)	0.55	0.28–1.10	0.09			
Pre-dilatation balloon maximum inflation pressure (1 atm increase)	1.06	0.95–1.18	0.32			
Maximum stent diameter (1 mm increase)	0.66	0.34–1.03	0.23			
Minimum stent diameter (1 mm increase)	0.67	0.35–1.28	0.23			
Stent implantation pressure (1 atm increase)	0.87	0.77–0.97	0.016	0.90	0.79–1.02	0.094
Post-dilatation balloon maximum diameter (1 mm increase)	0.68	0.37–1.26	0.22			
Post-dilatation balloon maximum inflation pressure (1 mm increase)	0.98	0.89–1.07	0.66			
Type of stent						
Second-generation drug-eluting stent	1.0 (reference)					
Third-generation drug-eluting stent	1.64	0.68–3.96	0.27			
Newer generation drug-eluting stent	1.57	0.38–6.43	0.53			
Drug-coated stent	2.00	0.89–4.50	0.09			
OCT findings immediately after PCI						
Incomplete stent apposition	0.73	0.39–1.36	0.73			
Malapposition volume (1 mm^3 increase)	0.89	0.77–1.02	0.097			
Maximum strut-to-vessel distance (1 mm increase)	0.39	0.11–1.39	0.15			
% malapposed struts (1% increase)	0.86	0.75–0.97	0.015	0.87	0.76–0.99	0.029
Minimum stent area (1 mm^2 increase)	0.92	0.70–0.96	0.015	0.89	0.75–1.05	0.172
Stent expansion index	2.23	0.40–12.43	0.36			
Underexpansion	0.72	0.39–1.35	0.31			
In-stent dissection	0.68	0.37–1.23	0.22			
Proximal stent edge dissection	1.87	0.60–5.84	0.28			
Distal stent edge dissection	1.67	0.39–7.21	0.49			
In-stent tissue protrusion	1.12	0.50–2.49	0.78			
Smooth protrusion	1.10	0.55–2.20	0.79			
Disrupted fibrous tissue protrusion	0.79	0.43–1.45	0.45			
Irregular protrusion	0.79	0.43–1.45	0.45			
Thrombus	0.54	0.22–1.31	0.17			

BMI body mass index; *CI* confidence interval; *CRP* C-reactive protein; *LDL* low-density lipoprotein; *OCT* optical coherence tomography; *OR* odds ratio; *PCI* percutaneous coronary intervention

[a]At the time of CAS follow-up

Table 4 Logistic regression analysis for subclinical intrastent Thrombus

	Univariate			Multivariate		
	OR	95% CI	*p*-value	OR	95% CI	*p*-value
Male	2.13	0.44–10.29	0.35			
Age (1 year increase)	1.01	0.98–1.05	0.49			
BMI (1 kg/m^2 increase)	0.99	0.89–1.10	0.83			
Hypertension	1.42	0.63–3.18	0.39			
Dyslipidemia	0.95	0.41–2.17	0.89			
Diabetes mellitus	1.02	0.52–2.02	0.95			
HbA1c (1% increase)	0.92	0.66–1.27	0.60			
LDL-Cholesterol (1 mg/dl increase)	0.99	0.98–1.00	0.12			
CRP (1 mg/dl increase)	3.40	1.06–10.90	0.04			
HbA1c at follow-up phase (1% increase)	1.08	0.80–1.46	0.61			
LDL-Cholesterol at follow-up phase (1 mg/dl increase)	0.99	0.98–1.01	0.38			
CRP at follow-up phase (1 mg/dl increase)	1.28	0.17–9.71	0.81			
Aspirin[a]	0.70	0.18–2.70	0.61			
Clopidogrel[a]	0.93	0.34–2.55	0.89			
Prasugrel[a]	0.80	0.35–1.86	0.61			
Ticlopidine[a]	1.26	0.11–14.25	0.85			
Statin[a]	1.13	0.53–2.44	0.75			
Follow-up duration (1 day increase)	1.00	0.99–1.01	0.22			
Acute coronary syndrome	1.94	0.69–5.45	0.21			
Pre-dilatation balloon maximum diameter (1 mm increase)	1.39	0.66–2.93	0.39			
Pre-dilatation balloon maximum inflation pressure (1 atm increase)	0.93	0.83–1.05	0.24			
Maximum stent diameter (1 mm increase)	1.08	0.51–2.27	0.85			
Minimum stent diameter (1 mm increase)	1.25	0.61–2.53	0.54			
Stent implantation pressure (1 atm increase)	0.92	0.81–1.05	0.20			
Post-dilatation balloon maximum diameter (1 mm increase)	1.46	0.74–2.89	0.27			
Post-dilatation balloon maximum inflation pressure (1 mm increase)	1.01	0.91–1.12	0.86			
Type of stent						
Second-generation drug-eluting stent	1.0 (reference)					
Third-generation drug-eluting stent	0.95	0.33–2.71	0.92			
Newer generation drug-eluting stent	0.88	0.15–4.97	0.88			
Drug-coated stent	1.97	0.79–4.92	0.15			
OCT findings immediately after PCI						
Incomplete stent apposition	0.84	0.42–1.68	0.63			
Malapposition volume (1 mm^3 increase)	1.13	1.00–1.28	0.06			
Maximum strut-to-vessel distance (1 mm increase)	1.95	0.52–7.23	0.32			
% malapposed struts (1% increase)	1.08	0.96–1.21	0.20			
Minimum stent area (1 mm^2 increase)	1.08	0.91–1.27	0.38			
Stent expansion index	0.30	0.04–2.09	0.22			
Underexpansion	1.95	0.98–3.89	0.06			
In-stent dissection	0.70	0.35–1.37	0.29			
Proximal stent edge dissection	1.06	0.31–3.56	0.93			
Distal stent edge dissection	1.58	0.36–6.90	0.54			
In-stent tissue protrusion	0.84	0.35–2.00	0.69			
Smooth protrusion	0.86	0.40–1.85	0.70			
Disrupted fibrous tissue protrusion	1.48	0.75–2.92	0.26			
Irregular protrusion	0.56	0.28–1.13	0.11			
Thrombus	1.35	0.53–3.39	0.53			

BMI body mass index; *CI* confidence interval; *CRP* C-reactive protein; *LDL* low-density lipoprotein; *OCT* optical coherence tomography; *OR* odds ratio; *PCI* percutaneous coronary intervention

[a]At the time of CAS follow-up

Table 5 Logistic regression analysis for vulnerable stented segment (≥ grade 2)

	Univariate			Multivariate		
	OR	95% CI	*p*-value	OR	95% CI	*p*-value
Male	6.83	0.85–54.91	0.07			
Age (1 year increase)	0.98	0.94–1.01	0.17			
BMI (1 kg/m^2 increase)	0.96	0.87–1.06	0.43			
Hypertension	0.55	0.27–1.14	0.11			
Dyslipidemia	0.98	0.44–2.21	0.97			
Diabetes mellitus	1.21	0.62–2.33	0.58			
HbA1c (1% increase)	0.90	0.66–1.27	0.52			
LDL-Cholesterol (1 mg/dl increase)	1.00	0.99–1.01	0.58			
CRP (1 mg/dl increase)	2.13	0.74–6.17	0.16			
HbA1c at follow-up phase (1% increase)	0.78	0.56–1.08	0.14			
LDL-Cholesterol at follow-up phase (1 mg/dl increase)	1.01	1.00–1.03	0.05			
CRP at follow-up phase (1 mg/dl increase)	0.85	0.11–6.57	0.87			
Aspirin[a]	1.33	0.32–5.44	0.70			
Clopidogrel[a]	1.56	0.62–3.91	0.35			
Prasugrel[a]	0.59	0.26–1.32	0.20			
Ticlopidine[a]	4.35	0.39–49.1	0.23			
Statin[a]	0.93	0.45–1.92	0.84			
Follow-up duration (1 day increase)	0.99	0.99–1.00	0.28			
Acute coronary syndrome	1.55	0.56–4.32	0.40			
Pre-dilatation balloon maximum diameter (1 mm increase)	1.24	0.61–2.56	0.55			
Pre-dilatation balloon maximum inflation pressure (1 atm increase)	0.98	0.87–1.10	0.73			
Maximum stent diameter (1 mm increase)	1.14	0.56–2.33	0.72			
Minimum stent diameter (1 mm increase)	1.56	0.79–3.08	0.20			
Stent implantation pressure (1 atm increase)	1.11	0.98–1.26	0.09			
Post-dilatation balloon maximum diameter (1 mm increase)	1.03	0.53–1.99	0.94			
Post-dilatation balloon maximum inflation pressure (1 mm increase)	1.03	0.93–1.14	0.57			
Type of stent						
Second-generation drug-eluting stent	1.0 (reference)					
Third-generation drug-eluting stent	1.31	0.54–3.20	0.55			
Newer generation drug-eluting stent	0.76	0.17–3.45	0.72			
Drug-coated stent	0.59	0.24–1.32	0.19			
OCT findings immediately after PCI						
Incomplete stent apposition	0.65	0.34–1.26	0.20			
Malapposition volume (1 mm^3 increase)	1.03	0.95–1.11	0.54			
Maximum. strut-to-vessel distance (1 mm increase)	0.47	0.12–1.93	0.30			
% malapposed struts (1% increase)	0.99	0.88–1.12	0.91			
Minimum stent area (1 mm^2 increase)	1.03	0.88–1.21	0.70			
Stent expansion index	0.91	0.15–5.65	0.92			
Underexpansion	1.04	0.53–2.02	0.92			
In-stent dissection	1.33	0.70–2.55	0.39			
Proximal stent edge dissection	0.32	0.07–1.50	0.15			
Distal stent edge dissection	0.69	0.14–3.55	0.66			
In-stent tissue protrusion	0.88	0.38–2.05	0.77			
Smooth protrusion	1.31	0.61–2.80	0.49			
Disrupted fibrous tissue protrusion	1.43	0.74–2.73	0.29			
Irregular protrusion	0.82	0.43–1.58	0.55			
Thrombus	1.62	0.67–3.94	0.28			

BMI body mass index; *CI* confidence interval; *CRP* C-reactive protein; *LDL* low-density lipoprotein; *OCT* optical coherence tomography; *OR* odds ratio; *PCI* percutaneous coronary intervention

[a]At the time of CAS follow-up

Table 6 Difference of vascular response after DES implantation according to the stent types

	Second-generation DES ($n=36$)	Third-generation DES ($n=47$)	Newer generation DES ($n=10$)	Drug-coated stent ($n=75$)	p value
Sufficient neointimal coverage, n (%)	14 (38.9)	24 (51.1)	5 (50.0)	42 (56.0)	0.41
Subclinical intrastent thrombus, n (%)	9 (25.0)	10 (21.3)	2 (20.0)	27 (36.0)	0.23
Vulnerable stented segment, n (%)	13 (36.1)	20 (42.6)	3 (30.0)	18 (24.0)	0.18

DES drug-eluting stent

studies revealed that the yellow grade increased from the baseline to 1 year after DES implantation, which indicated the occurrence of neoatherosclerosis [29, 30], the incidence of neoatherosclerosis was pathologically similar between first-generation DESs and second-generation DESs [31]. It is unclear whether the status of yellow color grade 1 year after stent implantation in the present study reflected the underlying lipid plaque or neoatherosclerosis, but a vascular response after DES implantation would change the intravascular status and minimize the findings immediately after PCI, which contributed to the absence of an association between OCT findings immediately after PCI and vulnerable stented segment at 1 year in this study, contrary to the report by Miyoshi et al. We observed that the yellow color grade at 1 year, which predicts the future prognosis [32], could not be predicted by the OCT findings immediately after stent implantation.

Limitations

This study has several limitations. First, it was a single-center, non-randomized observational study. Second, in some cases, the use of CAS could not completely evaluate the whole stented segments due to limitations in the visual field of the CAS, especially in angulated or tortuous lesions. However, in such cases, changing the guidewire sometimes improved the visual field. Third, OCT would be more preferable device to evaluate the neointimal coverage than CAS, because it has a higher resolution power. However, in this retrospective observational study, since we extracted the data from the database of coronary angioscopy, we decided to use the angioscopic findings for the evaluation of arterial healing in the chronic phase. Fourth, since we used two types of angioscopic catheter for the observation at different times, we could not completely deny the possibility that the differences between both equipment affected the assessment of intrastent findings. Finally, although the sample size was comparable to those of previous CAS studies [25], it is possible that the present sample size was insufficient to detect the relationship between post-PCI OCT findings and 1-year CAS findings. Larger scale studies are necessary to reach any conclusion about this issue.

Conclusions

Malapposition immediately after PCI was negatively associated with sufficient NIC at 1 year, although no associations were detected between post-PCI OCT findings and subclinical intrastent thrombus or vulnerable stented segment.

Funding None.

Data availability Our study data will not be made available to other researchers for purposes of reproducing the results, due to institutional review board restrictions.

Declarations

Conflict of interest O. Iida has received remuneration from Boston Scientific Japan. T. Mano has received a research grant from Abbott Medical Japan. The remaining authors have no disclosures to report.

IRB information Name of the ethics committee: The Medical Ethics Committee of Kansai Rosai Hospital; Reference number: 18D060g.

References

1. Tada T, Byrne RA, Simunovic I, King LA, Cassese S, Joner M, et al. Risk of stent thrombosis among bare-metal stents, first-generation drug-eluting stents, and second-generation drug-eluting stents: results from a registry of 18,334 patients. J Am Coll Cardiol Intervent. 2013;6:1267–74.
2. Nakazawa G, Finn AV, Vorpahl M, Ladich ER, Kolodgie FD, Virmani R. Coronary responses and differential mechanisms of late stent thrombosis attributed to first-generation sirolimus- and paclitaxel-eluting stents. J Am Coll Cardiol. 2011;57:390–8.
3. Finn AV, Joner M, Nakazawa G, Kolodgie F, Newell J, John MC, et al. Pathological correlates of late drug-eluting stent thrombosis: strut coverage as a marker of endothelialization. Circulation. 2007;115:2435–41.
4. Guagliumi G, Sirbu V, Musumeci G, Gerber R, Biondi-Zoccai G, Ikejima H, et al. Examination of the in vivo mechanisms of late drug-eluting stent thrombosis: findings from optical coherence tomography and intravascular ultrasound imaging. J Am Coll Cardiol Intervent. 2012;5:12–20.
5. Ishihara T, Awata M, Fujita M, Watanabe T, Iida O, Ishida Y, et al. Very late stent thrombosis 5 years after implantation of a sirolimus-eluting stent observed by angioscopy and optical coherence tomography. J Am Coll Cardiol Intervent. 2013;6:e28–30.

6. Inoue T, Shinke T, Otake H, Nakagawa M, Hariki H, Osue T, et al. Neoatherosclerosis and mural thrombus detection after sirolimus-eluting stent implantation. Circ J. 2014;78:92–100.
7. Schwartz RS. Pathophysiology of restenosis: Interaction of thrombosis, hyperplasia, and/or remodeling. Am J Cardiol. 1998;81:14E-17E.
8. Awata M, Kotani J, Uematsu M, Morozumi T, Watanabe T, Onishi T, et al. Serial angioscopic evidence of incomplete neointimal coverage after sirolimus-eluting stent implantation: comparison with bare-metal stents. Circulation. 2007;116:910–6.
9. Kubo T, Imanishi T, Takarada S, Kuroi A, Ueno S, Yamano T, et al. Implication of plaque color classification for assessing plaque vulnerability: a coronary angioscopy and optical coherence tomography investigation. J Am Coll Cardiol Intervent. 2008;1:74–80.
10. Mitsutake Y, Ueno T, Yokoyama S, Sasaki K, Sugi Y, Toyama Y, et al. Coronary endothelial dysfunction distal to stent of first-generation drug-eluting stents. J Am Coll Cardiol Intervent. 2012;5:966–73.
11. Räber L, Mintz GS, Koskinas KC, Johnson TW, Holm NR, Onuma Y, et al. Clinical use of intracoronary imaging. Part 1: Guidance and optimization of coronary interventions. An expert consensus document of the European Association of Percutaneous Cardiovascular Interventions. Eur Heart J. 2018;39:3281–300.
12. Kume T, Okura H, Miyamoto Y, Yamada R, Saito K, Tamada T, et al. Natural history of stent edge dissection, tissue protrusion and incomplete stent apposition detectable only on optical coherence tomography after stent implantation—preliminary observation. Circ J. 2012;76:698–703.
13. Ozaki Y, Okumura M, Ismail TF, Naruse H, Hattori K, Kan S, et al. The fate of incomplete stent apposition with drug-eluting stents: an optical coherence tomography-based natural history study. Eur Heart J. 2010;31:1470–6.
14. Gutierrez-Chico J, Wykrzykowska JJ, Nuesch E, van Geuns RJ, Koch K, Koolen JJ, et al. Vascular tissue reaction to acute malapposition in human coronary arteries: sequential assessment with optical coherence tomography. Circ Cardiovasc Interv. 2012;5:20–9.
15. Gutierrez-Chico JL, Regar E, Nuesch E, Okamura T, Wykrzykowska J, di Mario C, et al. Delayed coverage in malapposed and side-branch struts with respect to well-apposed struts in drug-eluting stents. Circulation. 2011;124:612–23.
16. Sanuki Y, Sonoda S, Muraoka Y, Shimizu A, Kitagawa M, Takami H, et al. Contribution of poststent irregular protrusion to subsequent in-stent neoatherosclerosis after the second-generation drug-eluting stent implantation. Int Heart J. 2018;59:307–14.
17. Soeda T, Uemura S, Park S-J, Jang Y, Lee S, Cho J-M. Incidence and clinical significance of poststent optical coherence tomography findings: one-year follow-up study from a multicenter registry. Circulation. 2015;132:1020–9.
18. Fujii K, Kubo T, Otake H, Nakazawa G, Sonoda S, Hibi K, et al. Expert consensus statement for quantitative measurement and morphological assessment of optical coherence tomography. Cardiovasc Interv Ther. 2020;35:13–8.
19. Kotani J, Awata M, Nanto S, Uematsu M, Oshima F, Minamiguchi H, et al. Incomplete neointimal coverage of sirolimus-eluting stents: angioscopic findings. J Am Coll Cardiol. 2006;47:2108–11.
20. Mitsutake Y, Yano H, Ishihara T, Matsuoka H, Ueda Y, Ueno T. Consensus document on the standard of coronary angioscopy examination and assessment from the Japanese Association of Cardiovascular Intervention and Therapeutics. Cardiovasc Interv Ther. 2021. https://doi.org/10.1007/s12928-021-00770-x.
21. Ishihara T, Tsujimura T, Okuno S, Iida O, Asai M, Masuda M, et al. Early- and middle-phase arterial repair following bioresorbable- and durable-polymer drug-eluting stent implantation: an angioscopic study. Int J Cardiol. 2019;285:27–31.
22. Okuno S, Ishihara T, Iida O, Asai M, Masuda M, Okamoto S, et al. Association of subclinical intrastent thrombus detected 9 months after implantation of 2nd-generation drug-eluting stent with future major adverse cardiac events—a coronary angioscopic study. Circ J. 2018;82:2299–304.
23. Nakamura D, Attizzani GF, Toma C, Sheth T, Wang W, Soud M, et al. Failure mechanisms and neoatherosclerosis patterns in very late drug-eluting and bare-metal stent thrombosis. Circ Cardiovasc Interv. 2016;9: e003785.
24. Taniwaki M, Radu MD, Zaugg S, Amabile N, Garcia-Garcia HM, Yamaji K, et al. Mechanisms of very late drug-eluting stent thrombosis assessed by optical coherence tomography. Circulation. 2016;133:650–60.
25. Lee SY, Ahn JM, Mintz GS, Hur SH, Choi SY, Kim SW, et al. Characteristics of earlier versus delayed presentation of very late drug-eluting stent thrombosis: an optical coherence tomographic study. J Am Heart Assoc. 2017;6: e005386.
26. Lee SY, Kim JS, Yoon HJ, Hur SH, Lee SG, Kim JW, et al. Early strut coverage in patients receiving drug-eluting stents and its implications for dual antiplatelet therapy: a randomized trial. J Am Coll Cardiol Imaging. 2018;11:1810–9.
27. Sakai S, Sato A, Hoshi T, Hiraya D, Watabe H, Ieda M. In vivo evaluation of tissue protrusion by using optical coherence tomography and coronary angioscopy immediately after stent implantation. Circ J. 2020;84:2235–43.
28. Miyoshi T, Kawakami H, Seike F, Oshita A, Matsuoka H. Relationship between yellow plaque grade and tissue protrusion after stent implantation: a coronary angioscopy study. J Cardiol. 2017;70:342–5.
29. Higo T, Ueda Y, Oyabu J, Okada K, Nishio M, Hirata A, et al. Atherosclerotic and thrombogenic neointima formed over sirolimus drug-eluting stent: an angioscopic study. J Am Coll Cardiol Imaging. 2009;2:616–24.
30. Akazawa Y, Matsuo K, Ueda Y, Nishio M, Hirata A, Asai M, et al. Atherosclerotic change at one year after implantation of endeavor zotarolimus-eluting stent vs everolimus-eluting stent. Circ J. 2014;78:1428–36.
31. Otsuka F, Vorpahl M, Nakano M, Foerst J, Newell JB, Sakakura K, et al. Pathology of second-generation everolimus-eluting stents versus first-generation sirolimus- and paclitaxel-eluting stents in humans. Circulation. 2014;129:211–23.
32. Ueda Y, Matsuo K, Nishimoto Y, Sugihara R, Hirata A, Nemoto T, et al. In-stent yellow plaque at 1 year after implantation is associated with future event of very late stent failure: The DESNOTE Study (Detect the Event of Very late Stent Failure From the Drug-Eluting Stent Not Well Covered by Neointima Determined by Angioscopy). J Am Coll Cardiol Intv. 2015;8:814–21.

Publisher's Note Springer Nature remains neutral with regard to jurisdictional claims in published maps and institutional affiliations.

Springer Nature or its licensor holds exclusive rights to this article under a publishing agreement with the author(s) or other rightsholder(s); author self-archiving of the accepted manuscript version of this article is solely governed by the terms of such publishing agreement and applicable law.